2019

A smartphone-based system for fluorescence polarization assays

Zijian Zhao
Iowa State University

A smartphone-based system for fluorescence polarization assays

by

Zijian Zhao

A thesis submitted to the graduate faculty

in partial fulfillment of the requirements for the degree of

MASTER OF SCIENCE

Co-majors: Electrical Engineering (Microelectronics and Photonics); Computer Science

Program of Study Committee:
Meng Lu, Co-major Professor
Jin Tian, Co-major Professor
Liang Dong

The student author, whose presentation of the scholarship herein was approved by the program of study committee, is solely responsible for the content of this thesis. The Graduate College will ensure this thesis is globally accessible and will not permit alterations after a degree is conferred.

Iowa State University

Ames, Iowa

2019

DEDICATION

I would like to thank my parents who have been supportive for my whole academic career and their guidance when I was suffered into hard times. And I would like to thank my girlfriend Weijia Su, who accompanies me all the time in ISU and helps me a lot during my graduate-student time.

TABLE OF CONTENTS

PAGE

NOMENCLATURE iv

ACKNOWLEDGMENTS v

ABSTRACT vi

CHAPTER 1. GENERAL INTRODUCTION 1

CHAPTER 2. LITERATURE REVIEW 5

CHAPTER 3. METHODOLOGY 8

CHAPTER 4. A SMARTPHONE-BASED SYSTEM FOR FLUORESCENCE POLARIZATION ASSAYS 16

CHAPTER 5. GENERAL CONCLUSION 35

APPENDIX. ADDITIONAL INFORMATION 36

NOMENCLATURE

FP	Fluorescence Polarization
FPIAs	Fluorescence Polarization Immunoassays
app	application
R6G	Rhodamine 6G
PBS	Phosphate Buffered Saline
PGE_2	Prostaglandin E2
LOD	Limit Of Detection

ACKNOWLEDGMENTS

I would like to thank the group of my POSC, Dr. Lu, Dr. Tian, and Dr. Liang. Dr. Lu is my major professor who discovered my talent and guided me through the project with patience. Dr. Tian is my co-major professor who instructed me with the computer science part in my project, and Dr. Liang gave me suggestions during the process of the project.

In addition, I would also like to thank my friends, colleagues, the department faculty and staff for making my time at Iowa State University a wonderful experience. I want to also offer my appreciation to those who were willing to participate in my surveys and observations, without whom, this thesis would not have been possible.

ABSTRACT

The purpose of this thesis is to perform fluorescence polarization(FP) analysis of biomolecules using a smartphone-based sensor. The FP detection can rapidly sense ligand-analyte bindings by measuring molecule mobility, and thus, FP-based assays have been widely used for rapid diagnostics in clinics.

Here, we implemented the FP detection apparatus using a 3D-printed compact holder and the built-in camera of a smartphone. The system offers accurate measurements of the degree of polarization by simultaneously detecting the fluorescence intensities parallel and perpendicular to the polarization of the excitation. The fluorescence signal of the sample is excited by a laser or light-emitting diode and separated by a polarization beam cube depending on the polarization. Parallel and perpendicular polarized emissions are projected onto two different regions of the sensor chip in the smartphone camera. A custom software app was developed to count the average intensity in the areas of interest and compute the degree of polarization. We validated the system by measuring the polarization of dye molecules dissolved in solutions with different viscosities. As an example of biomolecule sensing, a competitive FP immunoassay of Prostaglandin E2 was demonstrated using the developed system and exhibited the limit of detection of 1.57 ng/mL. The smartphone-based FP assay platform can also be implemented for the detection of toxins, disease biomarkers, and pathogens in resource-limited settings.

CHAPTER 1. GENERAL INTRODUCTION

1. Fluorescence Polarization Immunoassay

Fluorescence Polarization Immunoassay (FPIA) is a type of in vitro biochemical test which has been widely used for rapid detection of certain biomolecules in sample. And it is a competitive homogenous assay which is simple in terms of preparation and result demonstration. The basis of the assay is fluorescence anisotropy, also known as fluorescence polarization. If a fluorescent molecule is stationary and exposed to plane-polarized light, it will become excited and consequently emit radiation back to the polarized-plane. However, if the excited fluorescent molecule is in motion (rotational or translational) during the fluorescent lifetime, it will emit light in a different direction than the excitation plane. ("Fluorescence polarization immunoassay," 2019)

2. Smartphone-based System

smartphones, in conjunction with portable accessories, have been exploited for the in-vitro molecular diagnostics applications that have previously been available only to well-trained technicians using expensive analytical instruments (Hussain et al. 2017; Ludwig et al. 2015; Roda et al. 2016; Vashist et al. 2014; Xu et al. 2015; Zhang et al. 2015). For example, smartphone cameras have been adopted for several colorimetric detection assays, such as enzyme-linked immunosorbent assay, lateral flow immunoassay, and nanoparticle-based homogenous assays (Berg et al. 2015; Guler et al. 2017; Long et al. 2014; Ludwig et al. 2015; Wang et al. 2017; Wang et al. 2016). Attached to a compact spectrum analyzer, smartphones can be turned into compact readers for Raman spectroscopy and reflectometric label-free biosensors (Ayas et al. 2014; Cetin et al. 2014; Dutta et al. 2014; Gallegos et al. 2013; Liu et al. 2018). Furthermore, smartphone-based fluorescence detectors have been demonstrated for fluorescence-based DNA and protein

assays (Chen et al. 2017; Damhorst et al. 2015; Kuhnemund et al. 2017; Ludwig et al. 2015). These recent developments have been successfully implemented for pathogen detection, toxin detection, and disease diagnosis (Koydemir et al. 2015; Priye et al. 2017; Quesada-Gonzalez and Merkoci 2017; Wei et al. 2013). Using a smartphone, citizens with minimum training can carry out assays and thus facilitate the goal of point-of-need tests for in-vitro diagnosis.

3. Project Overview

This project demonstrates a smartphone-based FP detector that is capable of measuring the degree of polarization and thus detecting biomolecules. To obtain a compact FP detector, we implement a novel optical design that integrates a 3D printed housing and off-the-shelf optical components. The FP detector interfaces with smartphones through the built-in camera and a customized application (app). The compact FP detector can measure the degree of polarization with the performance comparable to a commercial laboratory fluorescence plate reader. The smartphone-based FP detection can be applied to most existing FPIAs. As an example, we demonstrate the quantification of a drug compound using a competitive FPIA. By combining the rapid, no-wash, and low-cost features of the FPIA and detector, the smartphone-based FPIA platform offers a promising solution for affordable bedside diagnostics.

4. Thesis Organization

This thesis consists of five chapters. Chapter one shows a big picture of this research where some important parts are briefly discussed. Chapter two reviews some literatures that are relevant to this research. Chapter three describes the methodology. Chapter four is the journal paper that has been published on *Biosensors and Bioelectronics.* Chapter five presents the general conclusion of the research.

References

Wikipedia contributors. (2019, August 9). Fluorescence polarization immunoassay. In *Wikipedia, The Free Encyclopedia*. Retrieved 22:17, October 8, 2019, from https://en.wikipedia.org/w/index.php?title=Fluorescence_polarization_immunoassay&oldid=910122657

Ayas, S., Cupallari, A., Ekiz, O.O., Kaya, Y., Dana, A., 2014. ACS Photonics 1 (1), 17-26.

Berg, B., Cortazar, B., Tseng, D., Ozkan, H., Feng, S., Wei, Q.S., Chan, R.Y.L., Burbano, J., Farooqui, Q., Lewinski, M., Di Carlo, D., Garner, O.B., Ozcan, A., 2015. ACS Nano 9 (8), 7857-7866.

Cetin, A.E., Coskun, A.F., Galarreta, B.C., Huang, M., Herman, D., Ozcan, A., Altug, H., 2014. Light Sci. Appl. 3 (1), e122.

Chen, W.L., Yu, H.J., Sun, F., Ornob, A., Brisbin, R., Ganguli, A., Vemuri, V., Strzebonski, P., Cui, G.Z., Allen, K.J., Desai, S.A., Lin, W.R., Nash, D.M., Hirschberg, D.L., Brooks, I., Bashir, R., Cunningham, B.T., 2017. Anal. Chem. 89 (21), 11219-11226.

Damhorst, G.L., Duarte-Guevara, C., Chen, W., Ghonge, T., Cunningham, B.T., Bashir, R., 2015. Engineering 1 (3), 324-335.

Duckworth, B.P., Aldrich, C.C., 2010. Anal. Biochem. 403 (1-2), 13-19.

Dutta, S., Choudhury, A., Nath, P., 2014. IEEE Photonic Tech. Lett. 26 (6), 568-570.

Flotow, H., Leong, C.Y., Buss, A.D., 2002. J. Biomol. Screen. 7 (4), 367-371.

Flower, R.J., Blackwell, G.J., 1976. Biochem. Pharmacol. 25 (3), 285-291.

Gallegos, D., Long, K.D., Yu, H., Clark, P.P., Lin, Y., George, S., Nath, P., Cunningham, B.T., 2013. Lab Chip 13 (11), 2124-2132.

Guler, E., Sengel, T.Y., Gumus, Z.P., Arslan, M., Coskunol, H., Timur, S., Yagci, Y., 2017. Anal. Chem. 89 (18), 9629-9632.

Hall, M.D., Yasgar, A., Peryea, T., Braisted, J.C., Jadhav, A., Simeonov, A., Coussens, N.P., 2016. Methods Appl. Fluoresc. 4 (2), 022001.

Hussain, I., Das, M., Ahamad, K.U., Nath, P., 2017. Sens. Actuators B Chem. 239, 1042-1050.

Jameson, D.M., Ross, J.A., 2010. Chem. Rev. 110 (5), 2685-2708.

Koydemir, H.C., Gorocs, Z., Tseng, D., Cortazar, B., Feng, S., Chan, R.Y.L., Burbano, J., McLeod, E., Ozcan, A., 2015. Lab Chip 15, 1284-1293.

Kuhnemund, M., Wei, Q.S., Darai, E., Wang, Y.J., Hernandez-Neuta, I., Yang, Z., Tseng, D., Ahlford, A., Mathot, L., Sjoblom, T., Ozcan, A., Nilsson, M., 2017. Nat. Commun. 8, 13913.

Lea, W.A., Simeonov, A., 2011. Expert Opin. Drug Discov. 6 (1), 17-32.

Liu, Q., Yuan, H., Liu, Y., Wang, J., Jing, Z., Peng, W., 2018. J. Biomed. Opt. 23 (4), 1-6.

Long, K.D., Yu, H., Cunningham, B.T., 2014. Biomed. Opt. Express 5 (11), 3792-3806.

Lucero, N.E., Escobar, G.I., Ayala, S.M., Paulo, P.S., Nielsen, K., 2003. J. Med. Microbiol. 52 (10), 883-887.

Ludwig, S.K.J., Tokarski, C., Lang, S.N., van Ginkel, L.A., Zhu, H.Y., Ozcan, A., Nielen, M.W.F., 2015. PloS One 10 (8), e0134360.

Moncada, S., Vane, J.R., 1978. Pharmacol. Rev. 30 (3), 293-331.

Priye, A., Bird, S.W., Light, Y.K., Ball, C.S., Negrete, O.A., Meagher, R.J., 2017. Sci. Rep. 7, 44778.

Quesada-Gonzalez, D., Merkoci, A., 2017. Biosens. Bioelectron. 92, 549-562.

Roda, A., Michelini, E., Zangheri, M., Di Fusco, M., Calabria, D., Simoni, P., 2016. Trends Anal. Chem. 79, 317-325.

Vashist, S.K., Mudanyali, O., Schneider, E.M., Zengerle, R., Ozcan, A., 2014. Anal. Bioanal. Chem. 406 (14), 3263-3277.

Volk, A., Kahler, C.J., 2018. Exp. Fluids. 59(5), 59-75.

Wang, L.J., Chang, Y.C., Sun, R.R., Li, L., 2017. Biosens. Bioelectron. 87, 686-692.

Wang, Y., Liu, X.H., Chen, P., Tran, N.T., Zhang, J.L., Chia, W.S., Boujday, S., Liedberg, B., 2016. Analyst 141 (11), 3233-3238.

Wei, Q.S., Qi, H.F., Luo, W., Tseng, D., Ki, S.J., Wan, Z., Gorocs, Z., Bentolila, L.A., Wu, T.T., Sun, R., Ozcan, A., 2013. ACS Nano 7 (10), 9147-9155.

Xu, X.Y., Akay, A., Wei, H.L., Wang, S.Q., Pingguan-Murphy, B., Erlandsson, B.E., Li, X.J., Lee, W., Hu, J., Wang, L., Xu, F., 2015. Proc. IEEE 103 (2), 236-247.

Zhang, D.M., Jiang, J., Chen, J.Y., Zhang, Q., Lu, Y.L., Yao, Y., Li, S., Liu, G.L., Liu, Q.J., 2015. Biosens. Bioelectron. 70, 81-88.

CHAPTER 2. LITERATURE REVIEW

1. Introduction

Smartphones have been perfectly adopted in our daily lives and these little devices can do much more than their regular functionalities. Incorporation of biosensing into smartphone platforms is a potentially powerful development, as biological assay capabilities that have previously only been available through expensive laboratory-based instruments may be utilized by anyone. Such developments may help to facilitate the goal of home-based tests may be used to diagnose a medical condition, but with a system that automatically communicates results to a cloud-based monitoring system that alerts the physician when warranted.

2. Smartphone-Based Sensors

Since their introduction in 1997 ‘‘smart’’ mobile phones with internet connectivity, high resolution cameras, touch screen displays, and powerful CPUs have gained rapid market acceptance. It is estimated that, there are 7.74 billion mobile phones that are currently in use (“HOW MANY PHONES ARE IN THE WORLD?”, 2019), 42.63% of them can be classified as smartphones, with an expected rise to 40% by 2020 (“61+ Revealing Smartphone Statistics for 2019”, 2019). The rapid acceptance of smartphones is driven by a combination of falling prices and increasingly sophisticated features. In addition, there is a growing ecosystem of applications that take advantage of the phone’s sensors, display, and connection to powerful computing and data storage capabilities that are available in the ‘‘cloud.’’ There is tremendous interest in transition laboratory-based biomolecular assays to mobile platforms that would enable disease diagnostics tests, pathogen detection, and toxin detection to be performed in point-of-use scenarios. Since the introduction of smartphones, hundreds of millions of the devices have been sold, with competition among platforms resulting in ever-increasing capabilities for computation, display,

and sensing. The built- in capabilities of smartphones can be further extended through the addition of accessories that enable the phone to sense different types of information. For example, it is already possible to find commercial lens systems that enable the phone to be used as a rudimentary microscope with 3506 magnification – sufficient for capturing images of cells, bacteria, and biological tissue (Gallegos et al. 2013). In each of these cases, the smartphone camera was used as a sensor to perform functions equivalent to much larger and more expensive laboratory instruments.

Low-cost portable biosensor systems integrated with smartphones may also enable diagnostic technology that can be translated to resource-poor regions of the world for pathogen detection, disease diagnosis, and monitoring of nutritional status. The ability of the smartphone camera to take images of the colored label components of a biological assay have been applied to lateral flow immunoassays (Zangheri et al. 2015) quantum-dot labeling of bacteria (Ming at al. 2015) and fluorescence micro- scopy (Wei et al. 2017). Furthermore, smartphone cameras have recently been exploited for microfluidic and optofluidic applications (Stemple et al. 2014) and as a lens-free microscopy tool (Zhang et al. 2016).

In particular, smartphone cameras developed for producing high pixel-count images and operating under low-light conditions have proven sufficient for fluorescence microscopy capable of observing individual fluorescent nanoparticles (Yu et al. 2014),detection of the output of photonic crystal biosensors (Gallegos et al. 2013), and colorimetric spectroscopy of colored liquids in enzyme linked immunosorbent assays (ELISA) (Berg et al. 2015). Such a system, deployed widely, would be capable of rapidly monitoring for the presence of environmental contaminants over large areas, or tracking the development of a medical condition throughout a large population. While ELISA-based biological assays can be applied to the detection of many biological analytes, their widespread adoption into scenarios outside the laboratory is hindered by the complexity of

the assay protocol, which involves the use of an enzyme-tagged secondary antibody and a color-generating substrate (Gallegos et al. 2013). Detection of an analyte through one of its intrinsic physical properties (dielectric permittivity, mass, conductivity, or Raman scattering spectrum – for example), called ‘‘label-free’’ detection (Gallegos et al. 2013), is preferable for assay simplicity in terms of the number of reagents required, washing steps needed, and assay time.

References

“HOW MANY PHONES ARE IN THE WORLD?” bankmycell, Nov, 2019, https://www.bankmycell.com/blog/how-many-phones-are-in-the-world

Deyang G. “61+ Revealing Smartphone Statistics for 2019” techjury, March 28, 2019, https://techjury.net/stats-about/smartphone-usage/#gref

Gallegos, D., Long, K. D., Yu, H., Clark, P. P., Lin, Y., George, S., ... & Cunningham, B. T. (2013). Label-free biodetection using a smartphone. Lab on a Chip, 13(11), 2124-2132.

Zangheri, M., Cevenini, L., Anfossi, L., Baggiani, C., Simoni, P., Di Nardo, F., & Roda, A. (2015). A simple and compact smartphone accessory for quantitative chemiluminescence-based lateral flow immunoassay for salivary cortisol detection. Biosensors and Bioelectronics, 64, 63-68.

Ming, K., Kim, J., Biondi, M. J., Syed, A., Chen, K., Lam, A., ... & Chan, W. C. (2015). Integrated quantum dot barcode smartphone optical device for wireless multiplexed diagnosis of infected patients. Acs Nano, 9(3), 3060-3074.

Wei, Q., Acuna, G., Kim, S., Vietz, C., Tseng, D., Chae, J., ... & Ozcan, A. (2017). Plasmonics enhanced smartphone fluorescence microscopy. Scientific reports, 7(1), 2124.

Stemple, C. C., Angus, S. V., Park, T. S., & Yoon, J. Y. (2014). Smartphone-based optofluidic lab-on-a-chip for detecting pathogens from blood. Journal of laboratory automation, 19(1), 35-41.

Zhang, Y., Wu, Y., Zhang, Y., & Ozcan, A. (2016). Color calibration and fusion of lens-free and mobile-phone microscopy images for high-resolution and accurate color reproduction. Scientific reports, 6, 27811.

Yu, H., Tan, Y., & Cunningham, B. T. (2014). Smartphone fluorescence spectroscopy. Analytical chemistry, 86(17), 8805-8813.

Berg, B., Cortazar, B., Tseng, D., Ozkan, H., Feng, S., Wei, Q., ... & Di Carlo, D. (2015). Cellphone-based hand-held microplate reader for point-of-care testing of enzyme-linked immunosorbent assays. ACS nano, 9(8), 7857-7866.

CHAPTER 3. METHODOLOGY

1. Introduction

Here, we implemented a system that is capable of measuring the full emission spectra of any light emitter (chemical fluorophore or quantum dot) and is thus capable of differentiating a broad range of tags. We demonstrated a simple interface to a conventional smartphone that enabled its internal camera to function as a high resolution and sensitive fluorescence spectrometer. By placing a transmission diffraction grating directly in front of the camera, along with optics for collimating light emitted from a liquid fluorescent sample onto the grating, an emission spectrum was distributed across the pixels of a complementary metal-oxide semiconductor (CMOS) image sensor with a single-pixel wavelength increment of 0.338 nm/pixel. We demonstrated that the smartphone fluorimeter is capable of performing a sensitive molecular- beacon FRET assay for a specific microRNA sequence with performance that is better than a conventional laboratory fluorimeter, with a detection limit, the lowest measured concentration that has an intensity value greater than three standard deviations above the negative control value, of 1.57 ng/ml. Our results showed that smartphone-based spectroscopic fluorimetry is a route toward portable biomolecular assays for viral/bacterial pathogens, disease biomarkers, and toxins, and this general-purpose approach may be extended to other photon-producing assay platforms such as FP, chemoluminescence, and fluorescent-tagged sandwich assays.

2. Material and Preparation

2.1 Materials and Reagents

Rhodamine 6G (R6G) and Coumarin 540A were purchased from Exciton (Oakley Inc. West Chester, OH, USA). Both R6G and Coumarin 540A were dissolved in methanol and then mixed with glycerol (Sigma-Aldrich, St. Louis, MO, USA). Reagents of PGE_2 FPIA kit (Catalog

ADI-920-001) were purchased from Enzo Life Sciences Inc. (Farmingdale, NY, USA). The kit contained a monoclonal PGE_2 antibody, assay buffer (tris buffered saline containing proteins and sodium azide), fluorescein conjugated PGE_2, and PGE_2 Standard (1,000 ng/ml PGE_2).

2.2 FP Detection Apparatus

The FP detection apparatus consists of an Android smartphone and a 3D-printed housing that interfaces with the rear-facing camera module of the smartphone. The housing was designed using Solidworks (Dassault Systems Inc., MA, USA) and printed by Shapeways Inc.(NY, USA) using acrylic with black finish. The housing holds and aligns all optical components including an excitation laser (DJ532-10 or L462P1400MM; Thorlabs Inc., NJ, USA), a collimation lens (LJ1402L1; Thorlabs Inc.), a linear polarizer (40-990; Edmund Optics Inc., NJ, USA), a plano-convex lens (LA154-A; Thorlabs Inc.), a polarizing beam splitter (49-001; Edmund Optics Inc.), two mirrors (43-790; Edmund Optics Inc.), and a bandpass filter (1005190B 109092 ILLM-0027, FF02-485/20-25, Semrock Inc). While holding all components in correct alignment, the black housing prevents stray light from reaching the camera. In this work, samples were measured in a micro quartz cuvette (Type 507, FireflySci Inc., ON, Canada) that can be inserted into the housing. Polystyrene cuvettes are incompatible due to the birefringence problem. The corresponding light wavelength information for all samples can be found in the following table (Table 1).

Table 1. Absorption/Emission Wavelength Overview

Sample	LED/Laser Wavelength(nm)	Emission Wavelength(nm)	Filter Wavelength(nm)
R6g	532	575	560-592
Coumarin 540A	462	550	520-560
Prostaglandin E2 (PGE_2)	462	520-535	520-560

To facilitate the design of the fluorescence detection optics, we utilized Lighttools (Synopsys Inc.) to simulate and optimize the optical imaging system (Figure S1, supporting information). In the assembled system, the collimation lens (focal length = 15 mm) is placed in from of the blue laser diode (λ = 462 nm and P_{max} = 1400 mW) or the diode pumped green laser diode (λ = 532 nm and P_{max} = 40 mW) to create a collimated beam with the beam diameter of d ~ 2 mm. The collimated laser beam is vertically polarized with the electric field along the z-axis (Figure 1(b)). The focusing lens (focal length = 15 mm) is set in front of the cuvette with the focal point at the center point of the excited volume inside the cuvette. Fluorescence light emerging from the excited volume is collected by the projection lens (focal length = 11 mm). When the fluorescent emission passes through the polarizing beam splitter, the signal beam is split to two beams depending on the polarization, as shown in Fig. 1(b). The vertical and perpendicular polarizations ($F_{//}$ and $F_{|}$) are reflected by the mirror, which oriented at a 30-degree angle with respect to the light

path. Two beams are projected on the internal CMOS sensor at different locations, enabling the analysis of the degree of polarization. The internal camera is sensitive to wavelengths within the visible spectrum, $400 < \lambda < 700$ nm. The width of the imaging spot is ~25 pixels.

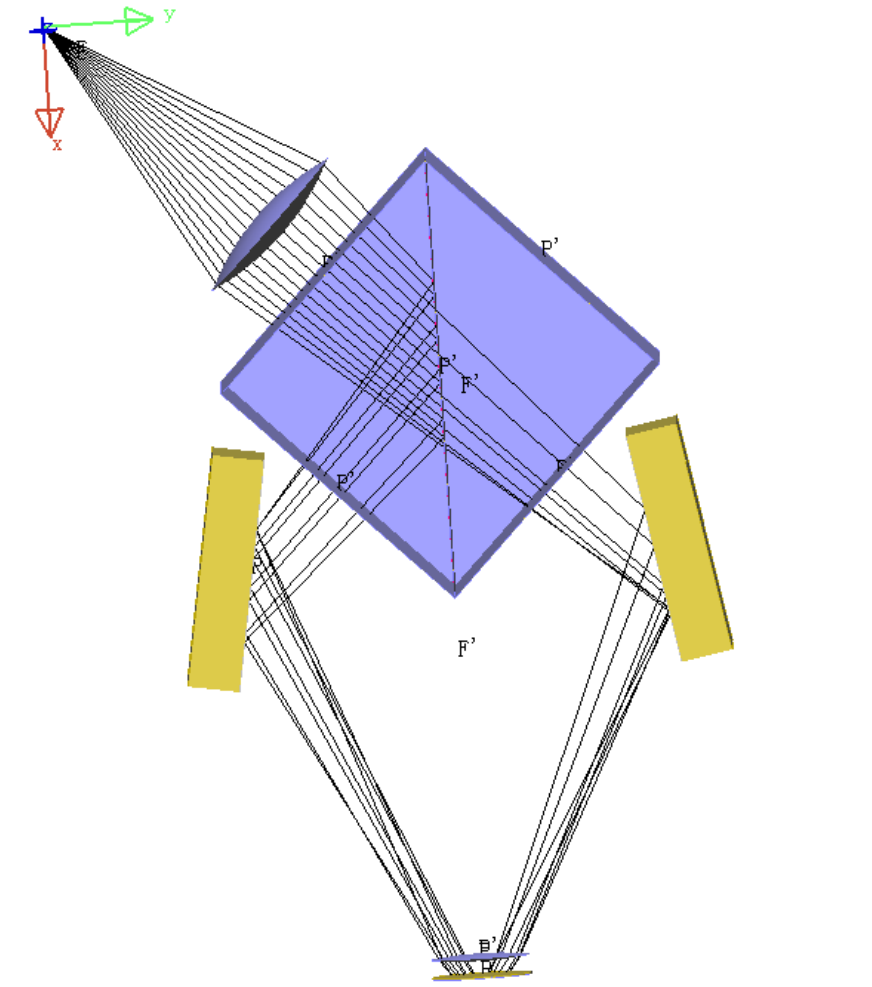

Figure 1. LightTools simulation

3. Fluorescence Anisotropic Tests

The smartphone-based FP detection system was tested using two proof-of-concept fluorescence anisotropic experiments. The degree of polarization (P) of two fluorescence dyes (Rhodamine 6G and Coumarin 540A) dissolved in solution with different viscosities was characterized. The fluorescent dyes were dissolved in ethanol with the concentration of 0.01 mg/mL and 0.01 mg/mL for Rhodamine 6G and Coumarin 540A, respectively. Glycerol was added in the dye solutions to adjust their viscosity. A series of samples with different amount of glycerol, from 0%, to 83% (v/v %), were prepared. These samples were measured to determine the fluorescence intensities ($I_{//}$ and $I_{\perp}$). The P value can be calculated using the following equation[9]:

$$P = \frac{I_{//} - I_{\perp}}{I_{//} + I_{\perp}}.$$

The degree of polarization of the samples were also measured using a laboratory desktop fluorimeter (Synergy 2 Multi-Mode Microplate Reader, BioTek).

4. FPIA Assay for PGE2

As an example of biomarker analysis, prostaglandin E2 (PGE_2) was chosen as the target molecule. PGE_2 is released by blood vessel walls in response to infection or inflammation that acts on the brain to induce fever. It has been proven that the PGE_2 has many biological actions such as vasodilation, both anti- and proinflammatory action, modulation of sleep/wake cycles, and facilitation of the replication of human immunodeficiency virus. The reagents of PGE_2 detection experiment were provided in the FPIA assay kit. Two sets of human IL-8 dilution series were measured using ELISA and PA immunoassays, respectively. The major steps involved in the immuno-sandwich assays are summarized in Fig. 2. The assays were performed in a microtiter

plate. The bottoms of the wells were coated with the IL-8 capture antibody and then blocked in a solution of BSA (1 mg/mL) in PBS for 1 h at room temperature.

Then we diluted 100 mL supplied Assay Buffer 1 concentration with 900 mL DI water, and labeled this to Assay buffer. Before preparing PGE2 Conjugate, we calculated the Conjugate Concentration by the flowing functions.

$$Vol_{assay\ buffer} = (Number\ of\ wells + 1) * 0.05\ mL/well$$

$$Vol_{PGE2\ Conjugate} = Vol_{assay\ buffer} * 10\ uL/mL$$

Then we pipetted Vol_{assay} buffer into a container and remove the $Vol_{PGE2Conjugate}$. Adding the calculated PGE_2 Conjugate concentrate to the assay buffer. Next step we pipetted 900 uL of assay buffer into a 12*75 tube and then label it to #1. After that we pipetted 500ul of assay buffer into other six same size tubes and labeled them #2 through #7. Afterwards, we took out the standard stock (1,000,000 pg/ml) and warmed it to room temperature. When standard solution was ready, 100ul of the solution was added into tube #1 and vortex thoroughly. Then, we added 500uL of tube #1 to tube #2 also vortex thoroughly. Continue this for tube#3 through #7. Finally, we got seven tubes of sample with different concentrations of PGE_2.

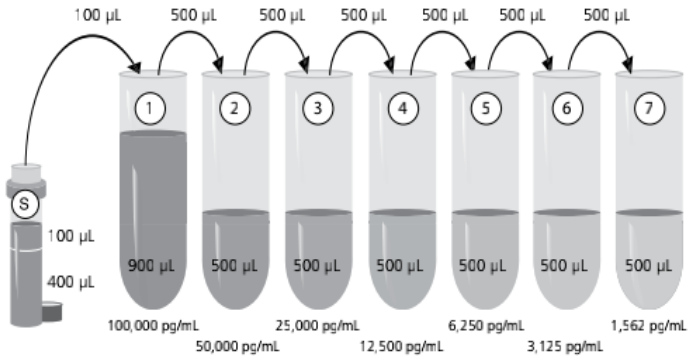

Figure 2. PGE2 Preparation

When all the standard solution and assay buffer were ready, we started to prepare the assays. 150 uL assay buffer was pipetted into the first well and labeled Total Fluorescence. Then we pipetted 100 uL of assay buffer into the second well and labeled it B_0(0 pg/mL), pipetted 100 uL of each standard solution to seven different wells and pipetted 100 uL of sample to another well. Afterwards we added 50uL conjugate into each well and added 50 uL antibody into each well (except the TF well). Lastly, we labeled all ten wells into one group and repeated the steps to prepare 8 groups for testing (Enzo Life Sciences Inc.).

5. Image Processing

When an ordinary digital photo is taken, the original image is divided into a grid as it is captured by the CMOS sensor. Pixels (the smallest resolvable grid spacing) are normally arranged in a two-dimensional grid, and each pixel of an image is a composite of three subpixels representing the red, green, and blue primary colors. The color information on each pixel is stored in 3 different multilayers of RGB color space. This results in a 2592 × 1936 × 3 matrix whose elements are real numbers ranging from 0 to 255 (8-bit number) for each digital color photo. However, when the camera is operated as a photodetector, we are only concerned with the total intensity gathered by all the subpixels because the hue information is spread over the screen as a color spectrum. Transformation from primary RGB colors to an HSV (Hue- Saturation-Value) color map was performed to provide a photon intensity of each pixel. HSV is a cylindrical coordinate representation of points in an RGB color space, where the V axis represents brightness of a corresponding color determined by V = Max (R, G, B). The values from our RGB image were converted into a V image in a 2592 × 1936 × 1 matrix of pixels.

Reference

Enzo Life Sciences Inc., 2018. PGE2 FPIA kit. http://www.enzolifesciences.com/ADI-920-001/pge2-fpia-kit/.

CHAPTER 4. A SMARTPHONE-BASED SYSTEM FOR FLUORESCENCE POLARIZATION ASSAYS

Zijian Zhao,[1] Le Wei,[1] Mingfeng Cao,[2] and Meng Lu[1,3,*]

[1]*Department of Electrical and Computer Engineering, Iowa State University, Ames, IA 50011*

[2]*Department of Chemical and Biomolecule Engineering, Iowa State University, Ames, IA 50011*

[3]*Department of Mechanical Engineering, Iowa State University, Ames, IA 500110.00*

Modified from a manuscript published in Journal Biosensors and Bioelectronics

Abstracts:

This paper demonstrates the use of a smartphone-based sensor for fluorescence polarization (FP) analysis of biomolecules. The FP detection can rapidly sense ligand-analyte bindings by measuring molecule mobility, and thus, FP-based assays have been widely used for rapid diagnostics in clinics. Here, we implemented the FP detection apparatus using a 3D-printed compact holder and the built-in camera of a smartphone. The system offers accurate measurements of the degree of polarization by simultaneously detecting the fluorescence intensities parallel and perpendicular to the polarization of the excitation. The fluorescence signal of the sample is excited by a laser or light-emitting diode and separated by a polarization beam cube depending on the polarization. Parallel and perpendicular polarized emissions are projected onto two different regions of the sensor chip in the smartphone camera. A custom software app was developed to count the average intensity in the areas of interest and compute the degree of polarization. We validated the system by measuring the polarization of dye molecules dissolved in solutions with

different viscosities. As an example of biomolecule sensing, a competitive FP immunoassay of Prostaglandin E2 was demonstrated using the developed system and exhibited the limit of detection of 1.57 ng/mL. The smartphone-based FP assay platform can also be implemented for the detection of toxins, disease biomarkers, and pathogens in resource-limited settings.

1. Introduction

Fluorescence polarization (FP) interrogates the polarization of light emitted by fluorophores, which are excited by a linearly polarized excitation (Ameloot et al. 2013; Jameson and Ross 2010; Lakowicz 2006). Since fluorophores are free to rotate in solution, the polarization of fluorescence emission within the fluorescence lifetime can point at a direction that differs from the polarization of the excitation light. The change of FP depends on the molecule's rotational speed and is associated with the solution's viscosity, temperature, and the size of fluorescent molecules. In particular, the size-dependent feature has been utilized to develop FP immunoassays (FPIAs) (Duckworth and Aldrich 2010; Flotow et al. 2002; Hall et al. 2016; Lea and Simeonov 2011; Lucero et al. 2003). Most FPIAs detect the change of FP caused by the binding of fluorophore bound ligand to the analyte of interest. As a homogenous assay, the FPIA eliminates multiple washing steps and only requires simple sample preparation and signal readout (Jameson and Ross 2010). Thus, the FPIA is suitable for the rapid detection of chemicals and biomolecules in resource-limited settings. Currently, expensive laboratory instruments are needed to measure FP signals. There is strong demand in using low-cost, compact, and portable systems to replace laboratory-based instruments.

Recently, smartphones, in conjunction with portable accessories, have been exploited for the *in-vitro* molecular diagnostics applications that have previously been available only to well-

trained technicians using expensive analytical instruments (Hussain et al. 2017; Ludwig et al. 2015; Roda et al. 2016; Vashist et al. 2014; Xu et al. 2015; Zhang et al. 2015). For example, smartphone cameras have been adopted for several colorimetric detection assays, such as enzyme-linked immunosorbent assay, lateral flow immunoassay, and nanoparticle-based homogenous assays (Berg et al. 2015; Guler et al. 2017; Long et al. 2014; Ludwig et al. 2015; Wang et al. 2017; Wang et al. 2016). Attached to a compact spectrum analyzer, smartphones can be turned into compact readers for Raman spectroscopy and reflectometric label-free biosensors (Ayas et al. 2014; Cetin et al. 2014; Dutta et al. 2014; Gallegos et al. 2013; Liu et al. 2018). Furthermore, smartphone-based fluorescence detectors have been demonstrated for fluorescence-based DNA and protein assays (Chen et al. 2017; Damhorst et al. 2015; Kuhnemund et al. 2017; Ludwig et al. 2015). These recent developments have been successfully implemented for pathogen detection, toxin detection, and disease diagnosis (Koydemir et al. 2015; Priye et al. 2017; Quesada-Gonzalez and Merkoci 2017; Wei et al. 2013). Using a smartphone, citizens with minimum training can carry out assays and thus facilitate the goal of point-of-need tests for *in-vitro* diagnosis.

This paper demonstrates a smartphone-based FP detector that is capable of measuring the degree of polarization and thus detecting biomolecules. To obtain a compact FP detector, we implement a novel optical design that integrates a 3D printed housing and off-the-shelf optical components. The FP detector interfaces with smartphones through the built-in camera and a customized application (app). The compact FP detector can measure the degree of polarization with the performance comparable to a commercial laboratory fluorescence plate reader. The smartphone-based FP detection can be applied to most existing FPIAs. As an example, we demosntrate the quantification of a drug compound using a competitive FPIA. By combining the

rapid, no-wash, and low-cost features of the FPIA and detector, the smartphone-based FPIA plateform offers a promissing solution for affordable bedside diagnostics.

2. Material and Methods

2.1 Materials and Reagents

Rhodamine 6G (R6G) and Coumarin 540A were purchased from Exciton (Oakley Inc. West Chester, OH, USA). Methanol, phosphate buffered saline (PBS), and glycerol were obtained from Sigma-Aldrich (St. Louis, MO, USA). Prostaglandin E2 (PGE2) FPIA kit (Catalog # ADI-920-001) was purchased from Enzo Life Sciences Inc. (Farmingdale, NY, USA). The FPIA kit contains a monoclonal PGE2 antibody, assay buffers, fluorescein-conjugated PGE2, and PGE2 standard sample.

2.2 FP Detection Apparatus

The underlying principle of FP analysis is illustrated in Figure 1(a), where the fluorescent molecules are excited by a linearly polarized light, and then the polarization of their fluorescent emission is analyzed. For molecules that rotate slowly with regard to the fluoresce lifetime, the emission is polarized. In contrast, the emission of fast rotating molecules become depolarized. The design of a compact FP analyzer (Figure 1(b)) can be implemented to determine the degree of polarization.

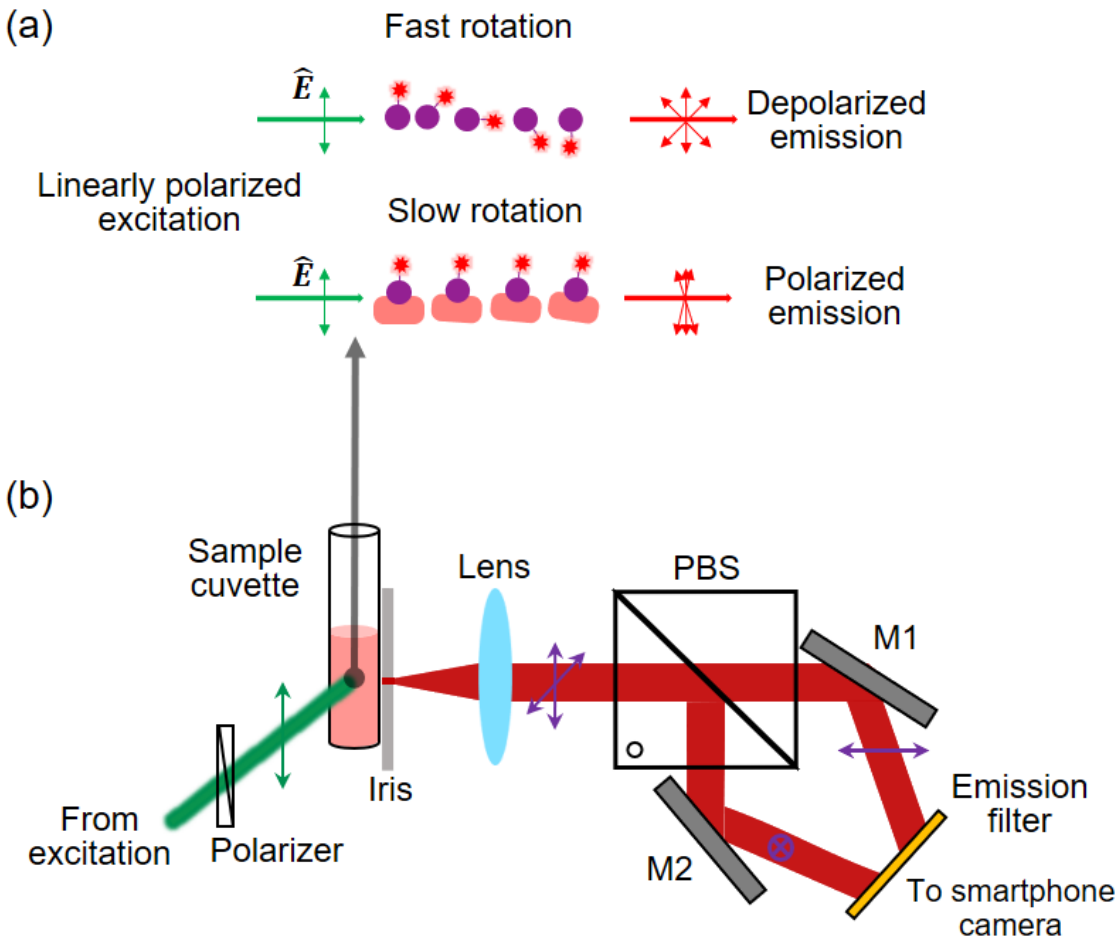

Figure 1. Schematics of the FP detection mechanism and optical setup. (a) Illustration of the FP assay. The fluorescence molecules are excited by a linearly polarized laser and the polarization state of the emission correlates to the rotation speed of the molecules. The binding with target molecules slows down the rotation and results in a more polarized emission. (b) The smartphone-based FP system setup consisting of a linearly polarized excitation, sample cuvette, iris, collection lens, polarizing beam splitter, two mirrors, emission filter, and smartphone camera.

The FP detection apparatus consists of a smartphone (HTC One M8 running Android 6.0) and a 3D-printed housing that contains optical components and can be attached to the rear camera of the smartphone. The housing of the FP detector was designed using SOLIDWORKS (Dassault Systems Inc., MA, USA) as shown in Figure 2(a). The housing was printed by Shapeways Inc.

(NY, USA) using acrylic with a black finish. Figure 2(b) shows the 3D-printed housing with all optical components including an excitation light source (DJ532-10 or L462P1400MM; Thorlabs Inc., NJ, USA), a collimation lens (LJ1402L1; Thorlabs Inc.), a linear polarizer (40-990; Edmund Optics Inc., NJ, USA), a plano-convex lens (LA154-A; Thorlabs Inc.), a polarizing beam splitter (49-001; Edmund Optics Inc.), two mirrors (43-790; Edmund Optics Inc.), and a bandpass filter (1005190B and FF02-485/20-25, Semrock Inc). The black surface finish and the cover prevent stray light from reaching the camera. In this work, a microfluorescence cuvette with the light path length of 3 mm (Type 507, FireflySci Inc.) was used to hold samples. The cuvette can be inserted into the housing to perform FP assays. The overall size of the fabricated housing is 98 mm × 60 mm × 58 mm.

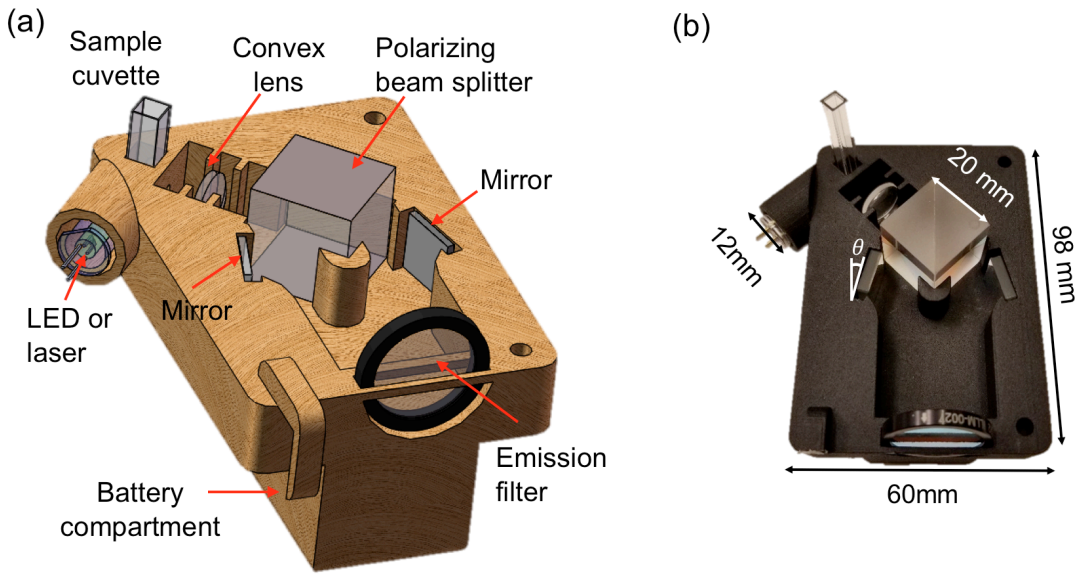

Figure 2. Diagram and photograph of the FP hardware. (a) Schematic design illustrating the housing and optics inside the FP detector. (b) Photograph of the 3D-printed housing and installed optical components. The total weight is less than 175 g. The cover part of the housing is not shown.

To design the FP detection optics, we utilized an optical design software (LightTools 8.5, Synopsys Inc.) to simulate and optimize the fluorescence imaging system that can measure two different polarizations simultaneously. In the assembled system, the collimation lens (focal length = 15 mm) is placed in front of the blue laser diode (λ = 462 nm and Pmax = 1400 mW) or the diode-pumped green laser source (λ = 532 nm and Pmax = 40 mW) to create a collimated excitation beam with the beam diameter of 2 mm. The excitation source can be easily installed and changed at the input port and are powered by the battery stored in the battery compartment as shown in Figure 2(a). The collimated laser beam is vertically polarized with the electric field along the z-axis (Figure 1(b)). During the 3D printing process, a pinhole (diameter of 1 mm) was created on the thin wall against the sample cuvette. The position of the pinhole is aligned at the center point of the excited volume inside the cuvette. A projection lens (focal length = 11 mm) collects fluorescent light emerging from the excited volume passing through the pinhole. Then, the fluorescent light is split into two beams depending on the polarization using the polarizing beam splitter cube, as shown in Figure 1(b). The vertical and horizontal polarizations (I// and I⊥) are reflected by the mirror, which is oriented at an angle of 30□ to the light path. To enable the analysis of the degree of polarization, two beams, representing I// and I⊥ emissions, are collected by the rear camera of the smartphone. As illustrated in Figure S1, the smartphone can be attached to the 3D-printed housing with its camera behind the emission filter. The emission filter, selected according to the fluorophore, can be inserted in the filter slot in front of the smartphone camera. The camera needs aligned to the fluorescent beams to image the beams at two different locations on the internal CMOS sensor, which is sensitive to visible light from 400 nm to 700 nm. The width of each fluorescent imaging spot is ~25 pixels.

2.3 Android app for Image Processing

The Android app was developed to capture images from the smartphone camera and calculate the degree of fluorescence polarization. The app functions as a graphic user interface that allows users to read and record assay results instantaneously. Images acquired from the CMOS sensor consists of 2592 × 1936 pixels (20 megapixels), and each pixel represents a 24-bit RGB color. As shown in Figure S2 of the supporting information, the app can identify the spots of vertically and horizontally polarized fluorescence and calculate the FP-value. For the sample with a low degree of polarization, the intensities of the spots are close, and vice versa. For both vertically and horizontally polarized spots, the intensities of red, green, and blue components are extracted, averaged, and displayed on the screen. The intensity of each channel ranges from 0 to 255. Since the fluorescence emissions usually fall within a given spectral band, the app calculates the FP-value based on the color channel specified by users.

2.4 Fluorescence Anisotropic Tests

The smartphone-based FP detection system was tested using two proof-of-concept fluorescence anisotropic experiments. The degree of polarization of two fluorescence dyes (Rhodamine 6G and Coumarin 540A) dissolved in solutions with different viscosities was characterized. The fluorescent dyes were dissolved in methanol with the concentration of 0.01 mg/mL for both Rhodamine 6G and Coumarin 540A samples. Glycerol was added in the dye solutions to adjust their viscosities. A series of samples with different amounts of glycerol, from 0% to 83% (v/v %) were prepared. Based on the volume ratio of the mixtures, the sample viscosity can be calculated (Cheng 2008; Volk and Kahler 2018). These samples were measured to determine the fluorescence intensities (I// and I⊥). The FP-value can be calculated using: $FP =$

$\frac{I_{//}-I_{\perp}}{I_{//}+I_{\perp}}$ (Ameloot et al. 2013). The degree of polarization of the samples was also measured using a laboratory desktop fluorimeter (Synergy 2 Multi-Mode Microplate Reader, BioTek).

2.5 FPIA Assay for PGE2

As an example, PGE2 was chosen as the analyte to demonstrate the quantitative FP analysis of biomarker using the smartphone platform. The reagents of PGE2 detection assay were provided in the FPIA assay kit. The assay was performed in the cuvette in a competitive manner. The first step is to add the PGE2 analyte with a volume of 50 μL into the cuvette. Then, a 25-μL fluorescein-conjugated PGE2 (10 μg/mL) was pipetted into the same cuvette and mixed with the unlabeled analyte. The mixture was incubated with a 25-μL of PGE2 specific antibody (10 μg/mL) for 30 minutes. And as a competitive immunoassay, the unlabeled analyte in the sample competes with the fluorescein labeled PGE2 to bind the PGE2 antibody. Hence, the amount of labeled and unbound PGE2 is proportional to the amount of analyte in the sample. After the incubation, the cuvette was inserted into the dongle and the FP results were read using the smartphone. The emission of fluorescein was excited using the blue laser diode and imaged through the green bandpass filter.

3. Results and Discussion

3.1 Fluorescence Anisotropy Measurement of Dyes

As a proof-of-concept experiment, we measured the FP-values of two organic dyes (Rhodamine 6G (R6G) and Coumarine 540) dissolved in methanol solutions with different viscosities. A sample with a high viscosity should exhibit a high degree of polarization since the

dye molecule rotation becomes slow. To adjust the sample viscosity, we added glycerol into the methanol solutions. At room temperature, the viscosities of glycerol and methanol are 1.41 Pa·s and 0.57 mPa·s, respectively. It is possible to control the sample viscosity by mixing glycerol and methanol at a desired percentage. The R6G and Coumarine 540 dyes have different absorption and emission signatures. The Android app and FP detector were slightly modified to measure the FP-values of both dyes. The details of the experiment, smartphone setup, and results are discussed as follows.

3.1.1 Fluorescence Anisotropy Measurement of R6G

The R6G dye is a highly efficient fluorophore with the absorption maximum and emission maximum located at approximately 530 nm and 575 nm, respectively. To measure the fluorescence emission of R6G, we installed the diode-pumped green laser ($\lambda_{ex} = 532$ nm) and the bandpass filter (560 nm < λ_{ex} < 592 nm) in the 3D-printed holder. Since the main portion of the R6G emission locates in yellow and red wavelengths, the Andriod app determines the spot intensities with only the red channel of acquired RGB images. To prepare the samples, we dissolved R6G in methanol at the concentration of 0.01 mg/mL and mixed the R6G-methanol solution with glycerol. For this experiment, 13 R6G samples were prepared to generate a series of viscosities with the glycerol concentration ranging from 0 to 83.33% (v/v, %). The corresponding viscosities of the samples are from 0.89 mPa·s to 97 mPa·s.

The fluorescence images of the samples with glycerol concentrations of 0%, 40%, and 80% are shown in Figure 3(a) from top to bottom. The exposure time was kept at 10 ms during the experiments. The red channel was extracted from the RGB images, and the averaged intensity in each fluorescent spot was calculated. For each concentration, the left and right spots represent the

vertically and parallelly polarized fluorescence emissions, respectively. The sample with a high concentration exhibits a more significant difference with regards to the spot intensity. To compare the I// and I⊥ quantitively, the intensity profiles along the dashed lines across both fluorescent spots in Figure 3(a) are compared in Figure 3(b). The sample without glycerol (red curve) shows nearly equivalent emissions for both polarizations. The increase of glycerol concertation results in the uneven emissions as shown in the yellow and blue curves. The FP-value reflects the degree of difference between the vertically and parallelly polarized emissions. Based on the averaged emission intensity in the left and right spots, the FP-values of the samples with 0%, 40%, and 80% glycerol are 0.08, 82, and 308.42 milli-polarization (mP), respectively.

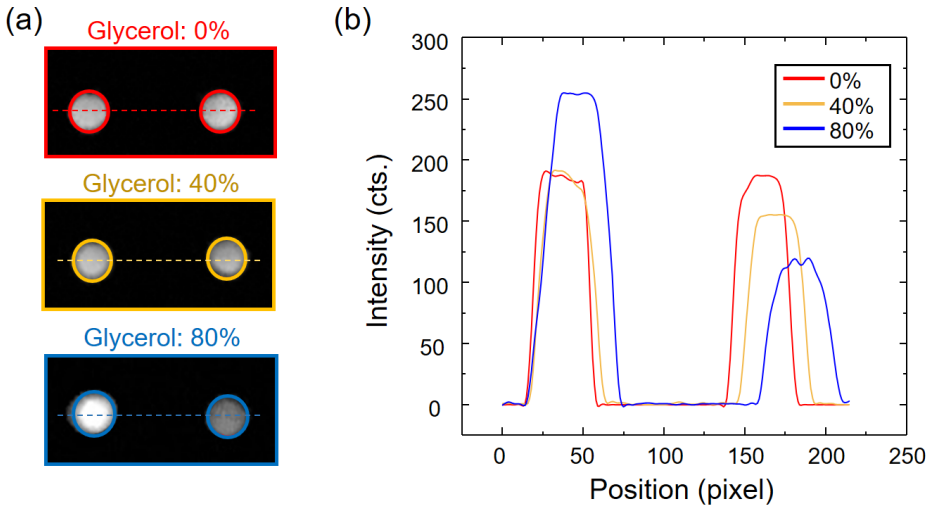

Figure 3. Analysis of FP-values for samples with different viscosities. (a) Beam spots for vertical (left spot) and horizontal (right spot) polarizations for the R6G solutions mixed with glycerol at the v/v ratio of 0%, 40%, and 80%, respectively. Only the red channels of the beam spots are shown. (b) Intensity profiles along the dashed lines shown in the images of beam spots. The beam intensities are plotted as a function of the CCD pixel.

The semi-log graphs in Figure 4 are plotted with a logarithmic scale on the x-axis representing the sample viscosity and a linear scale on the y-axis representing the FP-value with the unit of mP. The results in Figure 4(a) were measured using the smartphone-based FP detector. Measured data was fitted using the exponential function as shown by the red curve. The curve follows an exponential trend, and the polarization value reaches saturation when the sample viscosity is over 0.04 Pa·s. The linear response region is from 0.003 Pa·s to 0.041 Pa·s. For each viscosity, three replicated samples (n = 3) were measured and the coefficient of variation (C.V.) was calculated using C.V. = σ/μ, where σ and μ represent the standard deviation and mean values of the FP-values, respectively. To validate the smartphone-based system, we also measured the same samples using a commercial fluorescent plate reader (Synergy 2, BioTek). The results obtained by the benchtop reader are plotted in Figure 4(b). The response curves in Figure 4(a) and (b) match well.

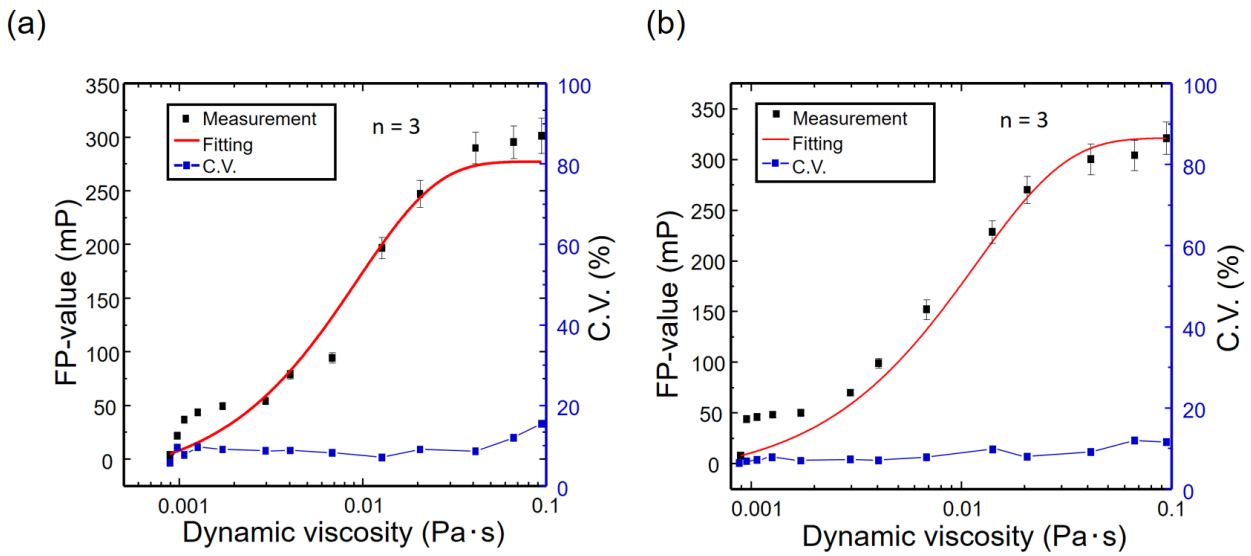

Figure 4. FP-values plotted as a function of the R6G sample viscosity. The FP response curve measured using the smartphone-based FP detector (a) and the benchtop plate reader (b). The FP-

values and C.V. numbers are shown by the left and right axes, respectively. The FP-values are fitted using exponential functions of $y = -299e^{-106.4x} + 277$ and $y = -338e^{-84.7x} + 321$ in (a) and (b), respectively. The error bar represents the standard deviation of the replicated samples.

3.1.2 Fluorescence anisotropy measure of Coumarin 540

The smartphone-based system can be implemented to measure FP signals emitted by many fluorophores. In addition to R6G, Coumarin 540 is a common organic dye, which has been widely used as the optical gain medium in dye lasers. The absorption and emission bands of Coumarin 540 locate at approximately 460 nm and 550 nm, respectively. The FP detector only needs to be slightly modified to measure the FP signals emitted by Coumarin 540. We replaced the green laser with a blue LED (λ_{ex} = 485 nm) and changed the bandpass filter to one with an emission band of 465 nm < λ_{ex} < 495 nm. Since the main portion of the Coumarin 540 emission locates in the green region, the app calculates the I// and I⊥ values based on the green channel of acquired RGB images.

Similar to the measurement of R6G samples, we prepared 13 samples with Coumarin 540 dissolved in methanol and different concentrations of glycerol. For each viscosity, three replicated samples were measured to calculate the C.V. numbers. The Coumarin 540 dye was dissolved in methanol at the concentration of 0.01 mg/mL. To generate the series of viscosities, we mixed the Coumarin 540 solution with the glycerol. The glycerol concentration and solution viscosity range from 0 to 83.3% (v/v, %) and from 0.89 mPa·s to 97 mPa·s, respectively. The semi-log plot in Figure 5 shows the measured polarization value as a function of sample viscosity. The FP curve of Coumarin 540 follows the same trend as the R6G test shown in Figure 5. The results of the FP analysis of organic dye solutions with different viscosities demonstrates the feasibility of using the smartphone system for FP-based analysis.

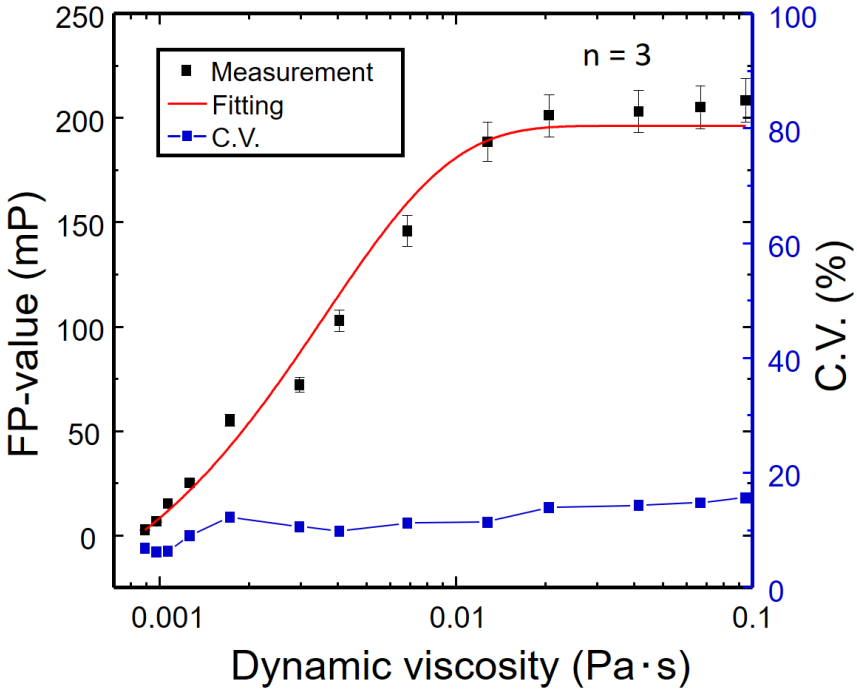

Figure 5. FP-values plotted as a function of the viscosity of Coumarin 540 solutions. The FP analysis of Coumarin 540 emission was performed using the green channel of the images acquired by the smartphone's CCD sensor. The FP-values and C.V. numbers are shown by the left and right axes, respectively. The measured result was fitted using an exponential curve ($y = -248e^{-277.8x} + 196.4$).

3.2 FPIA detection of PGE2

To determine the performance of the smartphone-based system for biomolecule analysis, the detection of PGE2 was performed using a competitive FP immunoassay. PGE2 is a bioactive lipid that is relevant to a wide range of biological effects. For example, PGE2 can be released by blood vessel walls in response to infection, inflammation, or cancer (Flower and Blackwell 1976; Moncada and Vane 1978). Here, the detection for PGE2 is performed in the manner of a

competitive homogeneous immunoassay, where analyte (unlabeled PGE2) competes with labeled PGE2 molecules to bind the PGE2-specific antibody. The binding of a fluorescein-conjugated PGE2 molecule to its antibody results in a slower rotation and consequently an increased FP-value. The presence of the analyte PGE2 competes with the labeled PGE2 and results in a smaller change of the FP-value. Therefore, the FP-value should be inversely proportional to the amount of analyte in the sample. The protocol of the competitive FPIA assay for PGE2 is summarized in Figure 6(a).

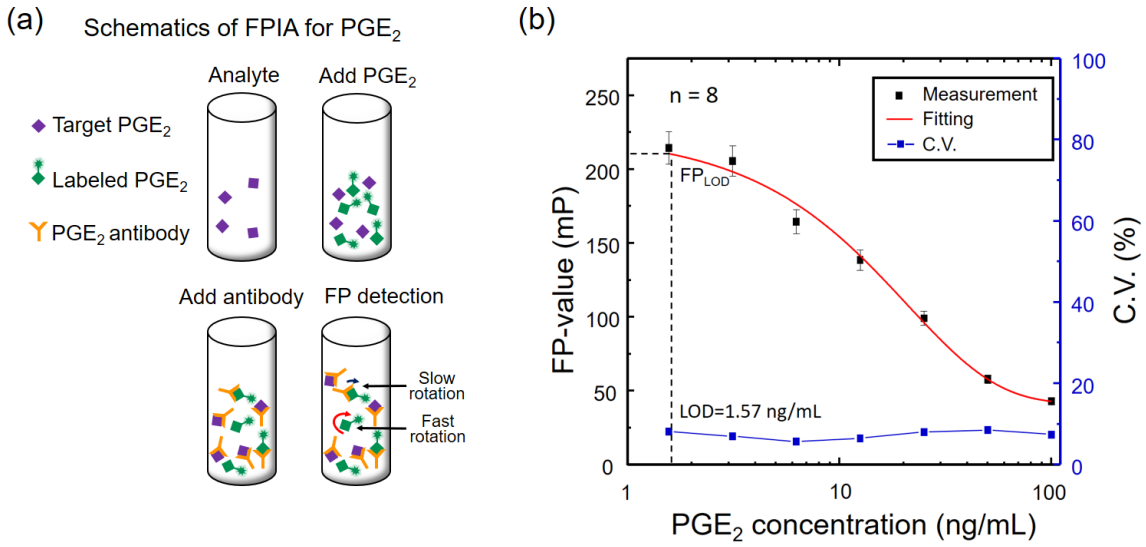

Figure 6. (a) Major steps of the FPIA detection assay for PGE2. As a competitive assay, the analyte is mixed with the fluorophore labeled PGE2 molecules and incubated with the PGE2 antibody. The presence of PGE2 consumes the antibody molecules and results in a higher number of the unbound, fast-rotation, and labeled PGE2. (b) Titration curve of PGE2 with the FP-values measured using the smartphone-based FP detector. The left and right axes show the FP-values and C.V. numbers, respectively. The data points are fitted using an exponential curve $y = 182e^{-\frac{x-1.3}{20684}} + 41.5$ shown in red.

To generate a titration curve for the analysis of PGE2, we prepared PGE2 samples at a series of seven concentrations ranging from 1.64 ng/ml to 100 ng/ml, with 2.5-fold dilutions and a reference sample without PGE2. For each PGE2 concentration, eight replicated samples were

prepared and measured. We measured the signal of a sample without the fluorescein conjugated PGE2 and used it as the background signal. The background signal was subtracted from the imaged fluorescent spots. The FP-values of all these samples were calculated and shown in Figure 6(b) as the dose-response curve. The measured curve correlates well with the results provided by the manufacture of the PGE2 FPIA kit (Enzo Life Sciences Inc.). The limit of detection (LOD) of the FPIA was calculated based on the FP-value that represents zero analyte concentration plus the three times of the standard deviation (FPLOD = FP0 + 3σ) (Taylor et al. 2001). For the detection of PGE2, the LOD value is 1.57 ng/mL (Figure 6(b)). It is worth noting that the proof-of-concept FPIA experiment used the PGE2 samples dissolved in PBS buffer without interfering molecules. Because of the limited selectivity of immunoassays, the LOD value may vary when PGE2 molecules are in a complex buffer, such as blood or urine, Here, we focus on the demonstration of the smartphone-based FP detector, rather than a particular FPIA detection.

4. Conclusions

This paper demonstrates a portable FP detection system that exploits the smartphone hardware to perform FPIAs. The FP detector, consisting of a 3D-printed housing and off-the-shelf optical components, can be attached to smartphones for a rapid FP analysis. The FP detector was prototyped with the total cost of $300 and weight of 175 g. We also developed a mobile app that functions as the user interface to facilitate the tests. Using two proof-of-concept experiments for red and green fluorescent dyes, we showed the system is capable of measuring FP states of the dye molecules and is identical to a commercial benchtop microplate reader. Furthermore, the smartphone based FPIA was implemented to detect PGE2 with a detection limit of 1.57 ng/mL. Owing to the benefits of portability and low cost, the smartphone-based FP detector can be adopted

as a point-of-care testing tool for a variety of chemicals and biomolecules, such as biomarkers, drug compounds, toxins, and metabolite products. For future work, we will explore the potentials in the following aspects. Firstly, a microfluidic chip will be integrated with the FP detector to enable multiplexed FP detections with minimized sample volume. The microfluidics chip will further reduce the assay time to meet the needs of rapid analysis for point-of-care testing. Secondly, we will add network connectivity to the mobile app in order to allow civilian users to share the FPIA results. Thirdly, the mobile FP technology in conjunction with FPIAs will be explored in potential fields, such as environmental monitoring and food safety in resource limited settings.

References

Ameloot, M., vandeVen, M., Acuna, A.U., Valeur, B., 2013. Pure Appl. Chem. 85 (3), 589-608.

Ayas, S., Cupallari, A., Ekiz, O.O., Kaya, Y., Dana, A., 2014. ACS Photonics 1 (1), 17-26.

Berg, B., Cortazar, B., Tseng, D., Ozkan, H., Feng, S., Wei, Q.S., Chan, R.Y.L., Burbano, J., Farooqui, Q., Lewinski, M., Di Carlo, D., Garner, O.B., Ozcan, A., 2015. ACS Nano 9 (8), 7857-7866.

Cetin, A.E., Coskun, A.F., Galarreta, B.C., Huang, M., Herman, D., Ozcan, A., Altug, H., 2014. Light Sci. Appl. 3 (1), e122.

Chen, W.L., Yu, H.J., Sun, F., Ornob, A., Brisbin, R., Ganguli, A., Vemuri, V., Strzebonski, P., Cui, G.Z., Allen, K.J., Desai, S.A., Lin, W.R., Nash, D.M., Hirschberg, D.L., Brooks, I., Bashir, R., Cunningham, B.T., 2017. Anal. Chem. 89 (21), 11219-11226.

Cheng, N.S., 2008. Ind. Eng. Chem. Res. 47 (9), 3285-3288.

Damhorst, G.L., Duarte-Guevara, C., Chen, W., Ghonge, T., Cunningham, B.T., Bashir, R., 2015. Engineering 1 (3), 324-335.

Duckworth, B.P., Aldrich, C.C., 2010. Anal. Biochem. 403 (1-2), 13-19.

Dutta, S., Choudhury, A., Nath, P., 2014. IEEE Photonic Tech. Lett. 26 (6), 568-570.

Flotow, H., Leong, C.Y., Buss, A.D., 2002. J. Biomol. Screen. 7 (4), 367-371.

Flower, R.J., Blackwell, G.J., 1976. Biochem. Pharmacol. 25 (3), 285-291.

Gallegos, D., Long, K.D., Yu, H., Clark, P.P., Lin, Y., George, S., Nath, P., Cunningham, B.T., 2013. Lab Chip 13 (11), 2124-2132.

Guler, E., Sengel, T.Y., Gumus, Z.P., Arslan, M., Coskunol, H., Timur, S., Yagci, Y., 2017. Anal. Chem. 89 (18), 9629-9632.

Hall, M.D., Yasgar, A., Peryea, T., Braisted, J.C., Jadhav, A., Simeonov, A., Coussens, N.P., 2016. Methods Appl. Fluoresc. 4 (2), 022001.

Hussain, I., Das, M., Ahamad, K.U., Nath, P., 2017. Sens. Actuators B Chem. 239, 1042-1050.

Jameson, D.M., Ross, J.A., 2010. Chem. Rev. 110 (5), 2685-2708.

Koydemir, H.C., Gorocs, Z., Tseng, D., Cortazar, B., Feng, S., Chan, R.Y.L., Burbano, J., McLeod, E., Ozcan, A., 2015. Lab Chip 15, 1284-1293.

Kuhnemund, M., Wei, Q.S., Darai, E., Wang, Y.J., Hernandez-Neuta, I., Yang, Z., Tseng, D., Ahlford, A., Mathot, L., Sjoblom, T., Ozcan, A., Nilsson, M., 2017. Nat. Commun. 8, 13913.

Lea, W.A., Simeonov, A., 2011. Expert Opin. Drug Discov. 6 (1), 17-32.

Liu, Q., Yuan, H., Liu, Y., Wang, J., Jing, Z., Peng, W., 2018. J. Biomed. Opt. 23 (4), 1-6.

Long, K.D., Yu, H., Cunningham, B.T., 2014. Biomed. Opt. Express 5 (11), 3792-3806.

Lucero, N.E., Escobar, G.I., Ayala, S.M., Paulo, P.S., Nielsen, K., 2003. J. Med. Microbiol. 52 (10), 883-887.

Ludwig, S.K.J., Tokarski, C., Lang, S.N., van Ginkel, L.A., Zhu, H.Y., Ozcan, A., Nielen, M.W.F., 2015. PloS One 10 (8), e0134360.

Moncada, S., Vane, J.R., 1978. Pharmacol. Rev. 30 (3), 293-331.

Priye, A., Bird, S.W., Light, Y.K., Ball, C.S., Negrete, O.A., Meagher, R.J., 2017. Sci. Rep. 7, 44778.

Quesada-Gonzalez, D., Merkoci, A., 2017. Biosens. Bioelectron. 92, 549-562.

Roda, A., Michelini, E., Zangheri, M., Di Fusco, M., Calabria, D., Simoni, P., 2016. Trends Anal. Chem. 79, 317-325.

Taylor, J., Picelli, G., Harrison, D.J., 2001. Electrophoresis 22 (17), 3699-3708.

Vashist, S.K., Mudanyali, O., Schneider, E.M., Zengerle, R., Ozcan, A., 2014. Anal. Bioanal. Chem. 406 (14), 3263-3277.

Volk, A., Kahler, C.J., 2018. Exp. Fluids. 59(5), 59-75.

Wang, L.J., Chang, Y.C., Sun, R.R., Li, L., 2017. Biosens. Bioelectron. 87, 686-692.

Wang, Y., Liu, X.H., Chen, P., Tran, N.T., Zhang, J.L., Chia, W.S., Boujday, S., Liedberg, B., 2016. Analyst 141 (11), 3233-3238.

Wei, Q.S., Qi, H.F., Luo, W., Tseng, D., Ki, S.J., Wan, Z., Gorocs, Z., Bentolila, L.A., Wu, T.T., Sun, R., Ozcan, A., 2013. ACS Nano 7 (10), 9147-9155.

Xu, X.Y., Akay, A., Wei, H.L., Wang, S.Q., Pingguan-Murphy, B., Erlandsson, B.E., Li, X.J., Lee, W., Hu, J., Wang, L., Xu, F., 2015. Proc. IEEE 103 (2), 236-247.

Enzo Life Sciences Inc., 2018. PGE2 FPIA kit. http://www.enzolifesciences.com/ADI-920-001/pge2-fpia-kit/.

Zhang, D.M., Jiang, J., Chen, J.Y., Zhang, Q., Lu, Y.L., Yao, Y., Li, S., Liu, G.L., Liu, Q.J., 2015. Biosens. Bioelectron. 70, 81-88.

CHAPTER 5. GENERAL CONCLUSION

In the project, we have demonstrated a smartphone based spectroscopic FPIA detector that is capable of performing valuable clinical assays in a portable system. Two proof-of-concept experiments using different dyes have been performed and by using a commercially available FPIA reagent for detection of a disease biomarker, we demonstrated limits of detection that are identical to or better than those obtained with a conventional FPIA microplate reader. Furthermore, we demonstrated that the spectral information available by measuring the entire absorption spectra of the assay liquid can be used to achieve a limit of detection of 1.57 ng/ml, compared to measuring the absorption at only a single wavelength. In addition to the benefits of portability and decreased cost, a smartphone FPIA platform also can make use of other smartphone capabilities, including immediate connectivity to the internet, geolocation, and has the potential for such results to be transmitted with medical records databases or even remotely located clinicians. Likely these capabilities can be further refined, and even translated to other spectroscopic assay modalities.

The resulting capability may find applications that include point-of-care detection/analysis of pathogens, specific nanoparticle detection, human/animal diagnostics, and food safety.

APPENDIX. ADDITIONAL INFORMATION

FP Detector Attached to a Smartphone

(a) (b)

Figure S1. (a) Schematic of the FP detector attached to a smartphone. The cover of the FP detector is not shown. The smartphone camera is aligned to the fluorescence emission beam. (b) Photography of the 3D-printed FP detector and smartphone. The LED is wired to a battery stored in the battery compartment.

Application User Interface

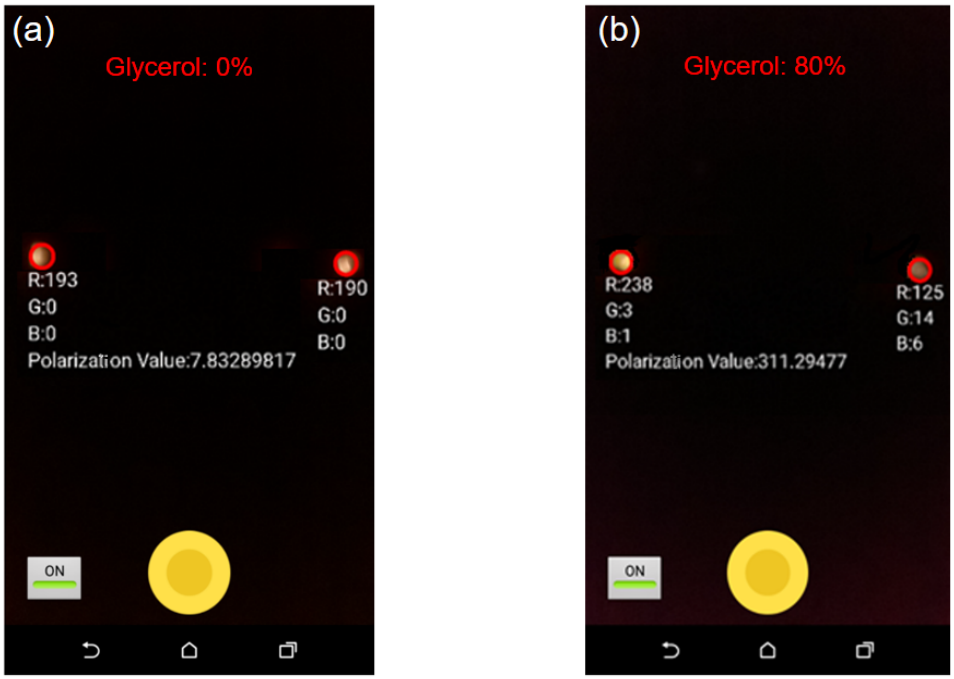

Figure S2. Android app for graphical user interface and data analysis. Two beams spots, representing the vertical and horizontal polarizations, are highlighted by the red circles. When a user presses the acquisition button (the yellow dot), the app can identify the beam spots, display the intensity for each of the RGB channels, and show the FP-value. (a) Fast rotation R6G molecules with unpolarized emission and the FP-value of 7.8. (b) Slow rotation R6G molecules show spots with a significant difference about their intensity.